

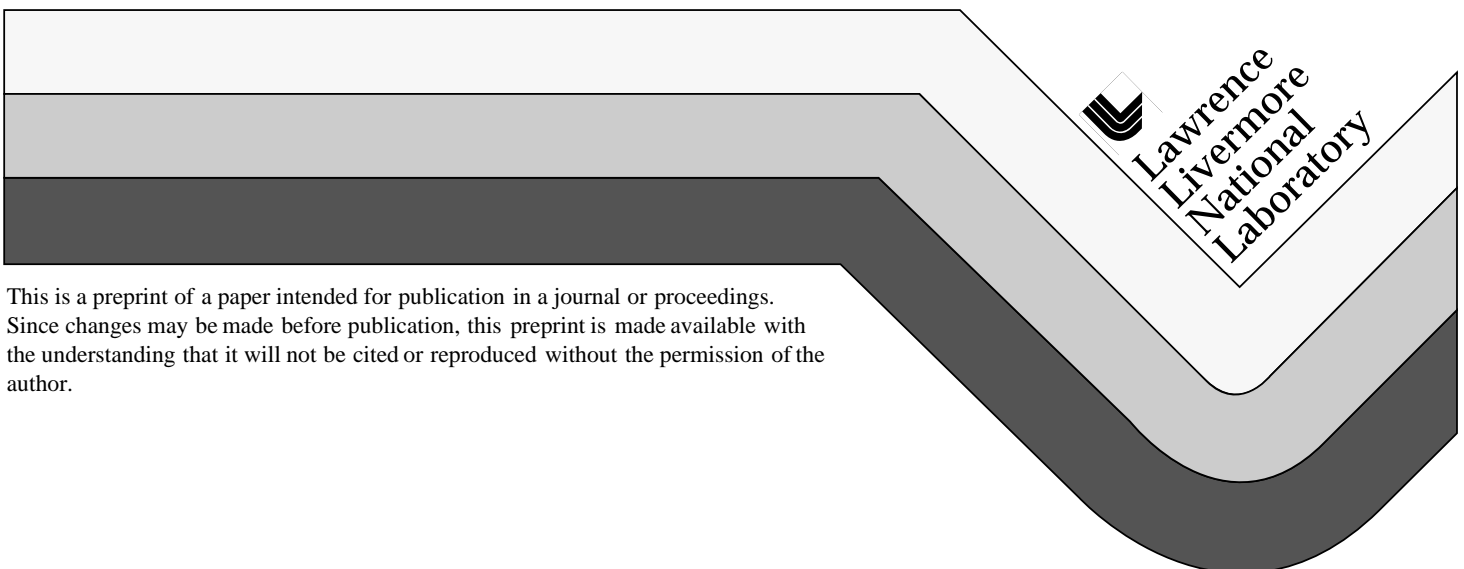
Plasma diagnostics for X-ray driven foils at Z

R.F.Heeter, J. Emig, M.E. Foord, P.T. Springer, and R.S. Thoe
Lawrence Livermore National Laboratory

J.E.Bailey and M.E.Cuneo
Sandia National Laboratories

This paper was prepared for submittal to
Review of Scientific Instruments

June 17, 2000



This is a preprint of a paper intended for publication in a journal or proceedings.
Since changes may be made before publication, this preprint is made available with
the understanding that it will not be cited or reproduced without the permission of the
author.

DISCLAIMER

This document was prepared as an account of work sponsored by an agency of the United States Government. Neither the United States Government nor the University of California nor any of their employees, makes any warranty, express or implied, or assumes any legal liability or responsibility for the accuracy, completeness, or usefulness of any information, apparatus, product, or process disclosed, or represents that its use would not infringe privately owned rights. Reference herein to any specific commercial product, process, or service by trade name, trademark, manufacturer, or otherwise, does not necessarily constitute or imply its endorsement, recommendation, or favoring by the United States Government or the University of California. The views and opinions of authors expressed herein do not necessarily state or reflect those of the United States Government or the University of California, and shall not be used for advertising or product endorsement purposes.

Plasma Diagnostics for X-Ray Driven Foils at Z

R. F. Heeter*, J. E. Bailey[†], M. E. Cuneo[†], J. Emig*, M. E. Foord*, P. T. Springer*, and

R. S. Thoe*

**Lawrence Livermore National Laboratory* P. O. Box 808, Livermore CA 94550*

[†]Sandia National Laboratories, P. O. Box 5800, Albuquerque, NM 87185

(June 17, 2000)

Abstract

We report the development of techniques to diagnose plasmas produced by X-ray photoionization of thin foils placed near the Z-pinch on the Sandia Z Machine. The development of 100+ TW X-ray sources enables access to novel plasma regimes, such as the photoionization equilibrium. To diagnose these plasmas one must simultaneously characterize both the foil and the driving pinch. The desired photoionized plasma equilibrium is only reached transiently for a 2-ns window, placing stringent requirements on diagnostic synchronization. We have adapted existing Sandia diagnostics and fielded an additional gated 3-crystal Johann spectrometer with dual lines of sight to meet these requirements. We present sample data from experiments in which 1 cm, 180 eV tungsten pinches photoionized foils composed of 200Å Fe and 300Å NaF co-mixed and sandwiched between 1000Å layers of Lexan (CHO), and discuss the application of this work to benchmarking astrophysical models.

TBD

Typeset using REVTeX

*This work was performed under the auspices of the U.S. Department of Energy by University of California Lawrence Livermore National Laboratory under contract no. W-7405-Eng-48.

I. INTRODUCTION

The development of intense laboratory X-ray sources powered by imploding Z-pinch plasmas^{1,2} provides the scientific community with new experimental capabilities, which in turn lead to new diagnostic challenges. This paper summarizes recent work using the Z machine at Sandia National Laboratory to produce the first laboratory plasmas in photoionization equilibrium. We will outline the diagnostic challenges in these experiments, document techniques to resolve these challenges, and present a sample of the early results in this area.

The motivation for this work arises in X-ray astronomy, where the Chandra and XMM satellite telescopes are now producing data with greatly increased spectroscopic resolution. A large fraction of astrophysical X-ray sources are accretion-powered objects where a core X-ray source photoionizes the surrounding gas, which makes photoionized plasmas a topic of great interest.

The photoionization equilibrium represents the balance between the processes of photoionization and recombination, and occurs when the ratio of the X-ray flux to the electron density is sufficiently high. We are most interested in the low density regime where 3-body recombination may be neglected relative to 2-body recombination processes, such that

$$n_i \Gamma_{rad} \int_x^\infty S(E) \sigma_i(E) E^{-1} dE = n_e n_{i+1} \alpha_{i+1}. \quad (1)$$

Here n_i is the density of an ion species, n_e is the electron density, Γ_{rad} is the radiation flux, and the integral term uses the spectral shape $S(E)$ and photoionization cross section $\sigma_i(E)$ to determine the photoionization rate coefficient, while α_{i+1} is the recombination rate coefficient. One traditionally sets $\xi \equiv \frac{4\pi\Gamma_{rad}}{n_e}$ and it follows that in this regime the ionization balance $\frac{n_{i+1}}{n_i}$ and much of the physics of plasmas is determined by fundamental atomic physics data (σ, α), the spectral shape $S(E)$, and the photoionization parameter ξ ^{3,4}. However, these simple labels conceal a vast number of processes taking place at the atomic level, and accounting for them all in detail is a considerable computational challenge.

The usefulness of the data being obtained by Chandra and XMM depends upon the quality of the models used to interpret the data. A recent comparison of 5 major photoionization models at $\xi \approx 100$ erg cm/s yielded divergent results for the iron charge balance, with the predicted dominant charge state ranging from +12 to +22 in the various models⁵. These results were not improved over an earlier comparison of 4 models at $\xi = 150$ erg cm/s⁶. This poses a considerable problem for the X-ray astronomy community. Confidence in the models can be increased by benchmarking the model predictions directly against experimental data obtained in well diagnosed laboratory experiments under known plasma conditions, but such experiments have only recently become possible.

To achieve a high photoionization parameter ξ , one must maximize the X-ray flux on a given sample while minimizing the sample density. The Z Machine is perhaps the strongest laboratory X-ray source today, routinely producing upwards of 100 TW (10^{21} ergs/s) by driving 18 MA of electrical current through cylindrical arrays of 100–400 fine wires^{1,2}. Samples may be placed as close as 15 or 16 mm from the pinch center. Working in cylindrical geometry one finds that a 100 TW, 1 cm long pinch produces an X-ray flux at the sample in excess of 3×10^{19} ergs/s/cm², comparable to the X-ray flux just 1500 km from a neutron star with a luminosity of 10^{37} ergs/s. We have found that the 100 ns run-in time of the pinch provides time for a foil to “blow down” to 10^{-4} or less of solid density, enabling Z to produce photoionization regimes with $\xi \sim 100$ erg cm/s, comparable to conditions found in such accretion powered astrophysical objects as X-ray binaries and active galactic nuclei^{6,5}. The details of the photoionizing spectrum, plasma composition and plasma density are different in the lab versus in astrophysics, but all of these factors can be measured in the laboratory and accounted for in the modeling, and the fundamental physical processes governing the photoionization equilibrium remain the same. Since it is now possible to produce photoionized plasmas in the laboratory, the next challenge in benchmarking the models is to diagnose such plasmas.

II. EXPERIMENTAL OBJECTIVES AND DIAGNOSTICS

To benchmark the models, one must characterize the flux, spectrum (temperature) and uniformity of the pinch, photoionize a sample into an astrophysically interesting regime, and then measure the absorption and emission of the sample while simultaneously determining the sample density and temperature. Our basic experimental approach is shown in Figure 1.

Although reasonably straightforward in principle, there are several subtleties in this design. For instance, many models used in astrophysics are equilibrium models, so in order to get useful data from a time dependent experiment, the X-ray drive pulse must allow the sample enough time to come into equilibrium with the radiation field of the pinch. One must then produce time gated measurements of the sample in this “steady state” regime, before the X-ray pulse terminates. As described previously^{6,5}, the design issues have been addressed using 1-D and 2-D time dependent radiation hydrodynamics simulations with the LASNEX code⁷, and lead to a tamped-foil configuration with 200 Å of iron (the astrophysically interesting component) co-mixed with 300 Å of sodium fluoride (low-Z tracers for temperature diagnostics), sandwiched within 1000 Å layers of Lexan (C,H, and O). In this configuration the X-ray pulse allows the foil conditions to reach equilibrium from 2–4 ns after peak X-ray power. This 2 ns time window poses a key challenge for the diagnostics, since 2 ns is comparable to the timing jitter of the best trigger signals available for gating the diagnostics at Z.

The diagnostic requirements for this experiment can be met by adapting a subset of the existing Sandia diagnostics and fielding an additional LLNL spectrometer, as shown in Figure 2. With north at 0 degrees, the various diagnostic lines of sight (LOS's) are labeled in increments of ten degrees, i.e. LOS 5/6 is at 50/60 degrees clockwise from north.

The pinch is characterized from 3 of the 9 diagnostic lines of sight available at Z. The LOS 5/6 instruments view the pinch through a 6 mm wide slot in the current return can surrounding the wire array, and measure the total pinch power (flux) and spectrum (0.25 to 2.25 keV) as functions of time by two methods: an absolutely calibrated transmission

grating spectrometer (TGS) and an absolutely calibrated array of bolometers in conjunction with a set of filtered X-Ray diode detectors. A blackbody fit to the TGS spectrum gives the emission temperature of the pinch as a function of time, as well; this method works for the tungsten pinches used in these experiments, which have no spectral lines overlapping the L-shell iron region in which we are interested. The X-ray power and spectrum measured by these instruments is what drives the foil samples, and is therefore an essential input to the models being benchmarked.

A pinhole camera on LOS 9/10 views the pinch through a 3 mm wide by 6 mm wide hole in the current return can. This pinhole camera has up to 9 individual 2 ns gates, allowing a sequence of images to be obtained over the course of the pinch, establishing the pinch width and spatial uniformity. The instrument configuration uses 100 micron pinholes with a magnification of 1.7. For these experiments the “hard” X-ray filter set was used, sensitive only to photons above about 600 eV. In this configuration the line of sight contains a total of 12.7 microns of Be, 5 microns of CH, and 0.016 microns of Al⁸.

In addition, a time and space resolved streak camera on LOS 33 was used to characterize the pinch emission seen through a 6 mm wide slot. This instrument has 60 ps time resolution over a 25 ns streak period, and 200 micron space resolution over a field of view of 10 mm⁹. The slits may be oriented to resolve the pinch either radially (horizontally) or axially (vertically). The instrument has dual views, and the filters for this experiment were set at 3 microns of Al and 12.7 microns of Be, respectively; again sensitive to photon energies above 600 eV.

The sample foils are characterized from 3 lines of sight. As shown in Figure 2, up to 3 foils may be used on each experiment. The foils are precision manufactured by Luxel Corp. (Friday Harbor, WA), and different foil batches are identical to about 5% in material thickness for a given specification. The principal foils are on LOS 13/14 and LOS 21/22, and see the pinch through identical 8 mm wide slots in the current return can.

The principal foil diagnostic for these experiments is an LLNL Johann curved crystal spectrometer on LOS 21/22. It uses a 3-stripline microchannel plate detector with a single

2 ns gate, recorded with TMAX 3200 film; it was previously used in a rather different configuration for experiments on the Saturn Z-pinch facility at Sandia¹⁰. As fielded in these experiments, the three crystals are divided into two sightlines using a complex array of individually adjustable baffles. One sightline obtains an image of the pinch and the foil in absorption, spatially imaged in the vertical (axial) direction, using a KAP crystal and a 100 or 150 micron imaging slit with magnification of 1.5. The other sightline uses two crystals (1 KAP, 1 mica) to obtain the spatially integrated emission spectrum of the foil at LOS 13. The central Bragg angle for all crystals in these experiments was 32.4° with a spectral range of $\pm 4.6^\circ$ on either side, giving a spectral range of 12.4 Å to 16 Å for the KAP and 9.3 Å to 12 Å for the Mica. This is the region where L-shell iron radiates most strongly, and also where the principal emission lines from the H- and He-like states of the tracer elements Na and F are found. Light filters totalling 0.3 microns of Al and 1 micron of CH were used on this instrument.

In our initial experiments the foils were placed face-on to the pinch, standing vertically (like a door); in subsequent experiments the foils were oriented horizontally, edge-on to the pinch (like a table). In the edge-on configuration the Johann's vertical resolution along the absorption line of sight allows the expansion of the foil to be measured from the extent of the principal absorption lines in the imaging direction.

The emission spectrum measurements provide 2 possible means of determining the foil temperature; first, from the slope of the free-bound continuum (model independent), and second, from the relative intensities of various line ratios, particularly from the Na and F in the foil. It is therefore possible, in principle, to obtain the full set of required measurements from the foil with only the Johann spectrometer.

In addition to the spectrometer on LOS 21/22, a 4 standard Sandia single-crystal spectrometers were fielded on LOS 13/14, including a pair of time-integrated, spatially-resolved KAP convex cylindrical crystal spectrometers sensitive from 8 to 18 Å, a single-gate time-and-space resolved KAP spectrometer with a smaller spectral range, and a 7-gate spatially integrated KAP spectrometer. DEF and 2484 film were variously used on these instruments.

These spectrometers viewed the pinch and the LOS 13 foil in absorption. In particular the time-integrated spectrometers are especially reliable and provide useful data weighted towards the peak X-ray emission on nearly every shot.

The final line of sight used on these experiments, LOS 29/30, views only the foil on LOS 21/22 in emission. A transmission grating spectrometer disperses light onto an array of 16 diodes which continuously measure the spectrum from 100 to 900 eV. In addition, a single continuous spectrum is taken with a 2 ns gate. Meanwhile, a pinhole camera with 4 filters, unity magnification, and 4 time gates (2 ns each) obtains a total of 16 images of the foil in emission. For our experiments we used a 3 micron Al filter with a 200 micron pinhole, a 5 micron (later 10) CH filter (with 0.1 and then 0.2 microns of Al) with a 100 micron pinhole, an 1 micron (later 2) Ti and Cr filters with 200 micron pinholes¹¹. The filter thicknesses were increased in order to bring the sensitivity of the last three filters in line with the 3 micron Al filter. The Al filter was chosen because it is sensitive only to the elements in the foil. Aside from the pinch and foil, all components of the experiment which might be in a diagnostic sightline were coated with boron, boron carbide, or plastic (CH) in order to suppress all other sources of X-rays above 600 eV.

III. INITIAL RESULTS AND FUTURE WORK

A preliminary experiment was carried out at Z in September 1999^{6,5}, here we also discuss a second-generation carried out in May 2000. The 2-shot first experiment successfully diagnosed the pinch and qualified it as a photoionization driver with 120 TW of peak X-ray power and electron temperatures of 180 eV. These initial shots were the shakedown experiment for the foil diagnostics. All instruments save one were successfully gated during the desired 2 ns window on one shot or the other. The foil design was validated when L-shell iron lines and various F and Na lines were observed in both time-integrated and time-resolved (Johann) spectra from the foil.

Several shortcomings were also identified. The initial pinhole camera filters were unable

to detect the foil against a background of boron and carbon blowoff, so the foil density could not be determined. Also, the LLNL Johann spectrometer was difficult to align and produced spectra with unacceptably high background levels. This led to a complete redesign of the foils into the horizontal configuration described above and a doubling of several pinhole camera filters. The Johann’s alignment system was also upgraded, including a “pinch simulator” light source for validating the positioning of five individually-adjustable baffles, and an in-vessel alignment monitoring fiducial laser/videocamera system which also proved capable of videotaping the destruction of the target by the pinch (to be described in a future paper).

The second generation experiment included 5 ridealong shots and 4 dedicated shots, which enabled much better instrument timings to be obtained; on the final shot all instruments were gated within the 2 ns “Steady State” window. The pinch diagnostics continued to work reliably. Time resolved emission and absorption spectra were obtained for the foil with acceptable backgrounds and signal-to-noise ratios; well over 50 L-shell Fe, Na and F emission lines have been distinguished in these spectra. Both the pinhole camera and the Johann spectrometer were able to image the foil expansion to about 3 mm, for an electron density of less than $1.5 \times 10^{19} cm^{-3}$, and an estimated photoionization parameter $\xi \approx 75$. A detailed analysis of these results is beyond the scope of this paper.

In summary, these experiments have provided data for photoionized iron plasmas which is critically needed to benchmark the atomic/plasma models used to interpret X-ray astronomy data. Future work on this project will focus on four main areas. First, additional data analysis is needed, leading to the production of benchmark test cases for the modeling community. Second, improved diagnostics for the temperature in the photoionized plasma are needed. These could make use of either line ratios in the measured emission spectra, new, highly sensitive spectrometers looking at the slope of the free-bound continuum in the range 1.1 to 2.0 keV, or possibly Thomson scattering. We have begun exploring the free-bound continuum method, but we need to overcome the obstacle of creating a sufficiently sensitive spectrometer within the hostile Z environment. Thomson scattering will be challenging due to the small sample volume and low density.

A third area for future work is to improve the quality of the time-gated absorption spectrum. Issues here include hot spot formation in the pinch (causing nonuniform backlighting), low opacities, and a need for better (scratch-free) crystals. Spectroscopic crystals tend to have short lifetimes in the Z environment due to mechanical shocks and particulate debris. Fast-moving dust particles have been found to travel in disturbing abundance up 4 meter long sightlines, through 100 micron apertures and 2 micron thick Al/CH blast shields, and then to produce undesirable impact damage to the crystals. Larger inventories of crystals will be obtained before future campaigns.

The fourth area for future work which we mention here is the development of additional pinch and foil designs, to allow more detailed benchmarking of the plasma models through parameter scans in density (photoionization parameter) and atomic number. Related to this is the goal of obtaining higher resolution spectra over a broader range of wavelengths. One interesting possibility might involve the creation of a foil with approximately cosmic abundances of various elements, for direct simulation of actual astrophysical plasmas.

The authors especially thank T. Dimwoodie at Sandia for timing and data acquisition support. We also thank S. Breeze, C. Coverdale, C. Deeney, D. Jobe, S. Lazier, J. McGurn, J. McKenney, and the Z Machine operations team at Sandia for experimental support, and the LLNL LDRD program for financial support.

REFERENCES

- ¹ C. Deeney *et al.*, Phys. Rev. Lett. **81**, 4883 (1998).
- ² M. G. Haines *et al.*, Phys. Plasmas **7**, 1672 (2000).
- ³ C. B. Tarter, W. Tucker, and E. E. Salpeter, Astrophysical Journal **156**, 943 (1969).
- ⁴ B. Tarter and E. E. Salpeter, Astrophysical Journal **156**, 953 (1969).
- ⁵ R. F. Heeter *et al.*, in *Proc. 12th APS Topical Conference on Atomic Processes in Plasmas* (AIP Conference Proceedings Series, ADDRESS, 2000), to be published.
- ⁶ R. F. Heeter *et al.*, in *Atomic Data Needs for X-Ray Astronomy*, edited by M. A. Bautista, T. R. Kallman, and A. K. Pradhan (NASA, Goddard Space Flight Center, Greenbelt, MD, 2000), pp. 135–142.
- ⁷ G. B. Zimmermann and W. L. Kruer, Comments on Plasma Phys. and Cont. Fusion **2**, 85 (1975).
- ⁸ S. Breeze, Private Communication, 2000.
- ⁹ S. E. Lazier, Private Communication, 1999.
- ¹⁰ K. L. Wong *et al.*, Phys. Rev. Lett. **80**, 2334 (1998).
- ¹¹ J. Seaman, Private Communication, 2000.

FIGURES

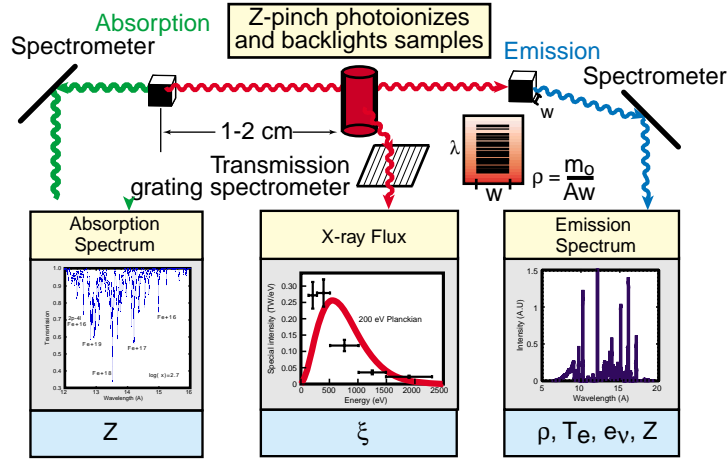


FIG. 1. Experimental Approach.

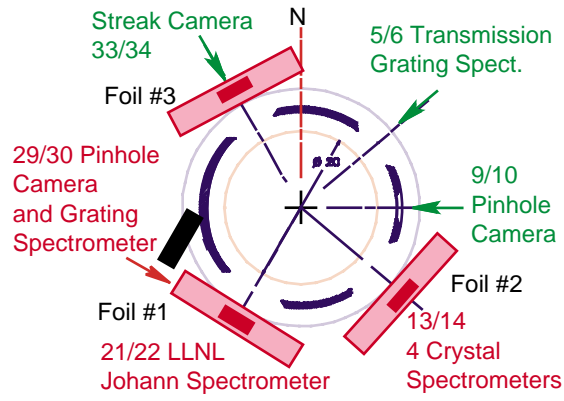


FIG. 2. Schematic of photoionization experiment, indicating relevant instrument lines of sight.

